A NOVEL IMAGE ENHANCEMENT METHOD FOR MAMMOGRAM IMAGES

A thesis presented to the faculty of the Graduate School of
Western Carolina University in partial fulfillment of the
requirements for the degree of Master of Science in Technology.

By

Hongda Shen

Director: Peter C. Tay, PhD
Assistant Professor
Department of Engineering and Technology

Committee Members:
James Z. Zhang, PhD
Department of Engineering and Technology
Robert D. Adams, PhD
Department of Engineering and Technology

March 2013

This thesis is dedicated to my parents who have supported me all the way since the beginning of my studies.

ACKNOWLEDGEMENTS

I am greatly thankful to my major advisor, Dr. Peter C. Tay, whose guidance, patient encouragement, and support from the initial to the final level enabled me to develop an understanding of the subject and the writing of this thesis. I am also grateful for Dr. James Z. Zhang and Dr. Robert D. Adams insightful criticisms and advice. Without any of these people's help, this thesis would not have been possible.

TABLE OF CONTENTS

LIST OF TABLES

LIST OF FIGURES

ABSTRACT

A NOVEL IMAGE ENHANCEMENT METHOD FOR MAMMOGRAM IMAGES

Hongda Shen, M.S.T.

Western Carolina University (March 2013)

Director: Peter C. Tay, PhD

Breast cancer has been reported by American Cancer Society as the second leading cause of death among all the cancers of women. It is also reported that the early detection of breast cancer can improve survival rate by allowing a wider range of treatment options. Mammography is believed to be an effective tool to help radiologists to detect the malignant breast cancer at the early stage. Image enhancement techniques can improve the quality of mammogram images with enhancing the details of key features, like the shape of microcalcifications. This thesis proposed a novel method to enhance mammogram images. The proposed method uses a three level Laplacian Pyramid (LP) scheme that applies the Squeeze Box Filter (SBF) instead of conventional low pass filtering. A previously proposed nonlinear local enhancement technique is applied to the difference image produced in the Laplacian Pyramid to contrast enhance the structural details of mammogram images. The enhanced mammogram image is reconstructed by adding all the enhanced difference images to the origianl SBF filtered image. Experimentation and quantitative results reported in this thesis provide empirical evidence on the robustness of the proposed image enhancement method on mammographic images.

CHAPTER 1: INTRODUCTION

This chapter discusses the general background and scope of this research, and concludes with the structure of this thesis.

1.1 Early Detection of Breast Cancer

The American Cancer Society (ACS) reports in 2013 that breast cancer ranks second as a cause of cancer death in women (after lung cancer). [1] Mammography can often detect breast cancer at an early stage, when treatment is more effective and a cure is more likely. Numerous studies have shown that early detection with mammography saves lives and increases treatment options. [1]

A concerning problem with mammography is the visual detection of early signs of breast cancer might be difficult especially in dense breast tissue. An example of a mammogram with pleomorphic and clustered microcalcifications (MCs) from the University of South Florida Digital Database of Screening Mammography (DDSM) [31] is shown in Fig. 1.1. The red outline in Fig. 1.1 is a radiologist defined region of interest (ROI). An early signs of potentially malignant breast cancer is the presence of at least one irregular shaped MCs. The ROI in Fig. 1.1 would be confirmed by biopsy as the site of a developing malignant breast cancer.

1.2 Objective

The objective of this thesis is to develop a robust image enhancement method to help radiologists visually detect irregular shaped MCs.

The proposed method in this thesis focuses on enhancing details and features like MCs that are not visibly well defined in the original image. Irregular shaped MCs can be a

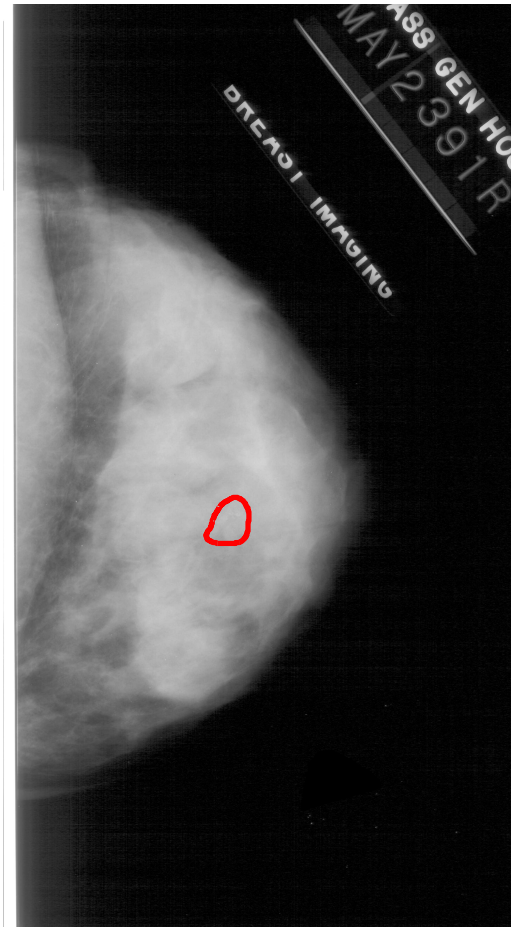

Figure 1.1: Mammogram with pleomorphic and clustered MCs. The radiologist defines ROI is shown as the red contour.

very good indicator of potential malignant breast cancer. [33]. Therefore, it is required that the enhancement techniques should not distort the shape of the features including MCs in mammogram images. The proposed enhancement technique is in essence a three level LP scheme. The SBF is used instead of low pass filtering in the typical LP and provides smooth frequency selective images because SBF has been proven to be a good approximation to the background of the mammogram images in [3]. Subtracting the SBF smoothed image from the original image will produce the difference image. After that, a previously proposed non-linear local contrast enhancement technique is applied to amplify features that were clouded in the original image without distorting edges. The final detail enhanced image is produced by summing the first level SBF image with all of the enhanced difference images.

The result is a contrast enhanced image with visually enhanced details. This proposed image enhancement method will be discussed in details in Chapter 3.

1.3 Structure of the Thesis

This thesis includes four chapters. The current state of the image enhancement methods will be review in the Chapter 2: Literature Review. The methodology Chapter will discuss the details of the proposed method in this research including SBF and its variant, Laplacian Pyramid, Nonlinear Functional Mapping and metric for measurement of image enhancement especially contrast enhancement. Experiments were done to prove the effectiveness of this new proposed method in the Chapter 4. Chapter 5 will give an detailed summary about what has been accomplished in this research and possible future research directions.

CHAPTER 2: LITERATURE REVIEW

In recent years, many image enhancement techniques have been developed to improve the quality of mammogram images [14, 16, 22–24]. In this thesis, "enhancement" refers to improving the contrast of the mammogram images without amplifying noise. In other words, denoising and contrast enhancement are the two major targets that I wish to achieve. However, it is not easy to enhance the contrast and remove the noise at the same time. In order to increase the radiologists' diagnostic accuracy, a good image enhancement should enhance the contrast of mammogram images and suppress the image noise simultaneously.

Contrast enhancement is one of the basic topics in image processing, pattern recognition and computer vision. Image processing researchers have developed various image enhancement algorithms. Histogram Equalization (HE) [13] is considered as the most widely used image contrast enhancement algorithm for its fast and easy implementation features. HE adjusts the intensity histogram to approximate an uniform distribution. Its variant version, Histogram Specification (HS) [13] can adjust intensity histogram to a predefined distribution. Although HE can enhance the contrast globally, it tends to over-enhance the image locally especially when there are large peaks in the histogram. In addition, the image noise may be enhanced by HE at the same time, which will produce unsatisfactory enhancement.

In contrast to conventional contrast enhancement approaches, like HE or HS, there is another group of algorithms which mainly focus on decomposing the original image into different subbands and then processing the magnitude of the desired frequency components of the image. Wavelet and Empirical Mode Decomposition (EMD) are two examples of this group of image enhancement methods. Many recent research works have proved that this type of algorithms can enhance the image globally and locally. However, noise

amplification problem still exists in these approaches.

The existence of noise in the mammographic images may reduce the breast cancer detection rate and accuracy. Therefore, noise needs to be suppressed while the structure of the mammographic images is enhanced. Nevertheless, most contrast enhancement algorithms enhance the image structure and noise simultaneously. In earlier time, researchers have developed some typical linear or nonlinear filters to denoise the signal. However, those conventional filters will produce edge blurring and loss of details. Currently, wavelet and EMD have already been used efficiently in image denoising. It is believed that noise is evenly distributed in the wavelet coefficients and those coefficients are relatively small. So hard and soft thresholding are used to remove those small wavelet coefficients in order to remove the image noise. A lot of research works have proved the effectiveness of wavelet methods to denoise the images. Also wavelet decomposition with thresholding method has been developed to enhance the mammographic images. [14]

EMD was first developed for analyzing nonstationary data. Now there are a growing number of researchers working on analyzing or processing various signal by EMD including signal denoising. [21] Although wavelet thresholding and EMD thresholding share very similar main principles, wavelet uses fixed basis functions while EMD derives the basis functions from the input signal. Curvelet and Contourlet are developed based on wavelet concept to fix some problems of wavelets and they work very well in certain applications.

2.1 Histogram Equalization

HE [13] is a useful and most commonly used tool to enhance the contrast of an image. The basic idea of HE method is to adjust the histogram of input image to a uniform one. Assume the input image has L grayscale level and N pixels. The probability of ith grayscale level is defined as following:

$$p(i) = \frac{n_i}{N} \quad i = 0, 1, 2, \cdots, L-1 \tag{2.1}$$

n_i here means the number of pixels whose grayscale level is i. The cumulative distribution function (CDF) $F(i)$is computed as:

$$F(i) = \sum_{k=0}^{i} p(k) \quad \text{and} \quad \sum_{k=0}^{L-1} p(k) = 1$$

Then the distribution of the pixel grayscale value will be mapped to a uniform distribution in order to enhance contrast of the image. The intensity transfer function maps all grayscale levels in the input image to new grayscale values in the enhanced images. Therefore, the intensity transfer function for HE is defined as:

$$T(i) = (L-1) \times \frac{\sum_{k=0}^{i} p(k)}{\sum_{k=0}^{L-1} p(k)} = (L-1) \times \sum_{k=0}^{i} p(k). \tag{2.2}$$

This transfer function will map all the grayscale values of original image to new grayscale values.

Figure 2.1 shows an example of HE. Fig 2.1a is the original image, Fig 2.1b is the enhanced image. Fig 2.1c and Fig 2.1d are corresponding histograms to Fig 2.1a and Fig 2.1b respectively. The contrast of the Fig 2.1b image is enhanced by a more uniform histogram.

Intuitively, a large peak in the histogram causes a steep increase in the CDF. Hence, over-enhancement happens because of these large peaks. Over-enhancement may cause the loss of detail in medical images especially in mammographic images. Another drawback of HE is the noise of images may be enhanced at the same time.

To overcome these drawbacks of HE method, many other algorithms have been developed to improve HE. The conventional HE method is a global technique. Then researchers developed a local histogram equalization [5] which uses a moving window centered at each pixel to equalize the local histogram, which solve over-enhancement problem to some extent. Q.Wang et.al. [6] proposed a new histogram equalization algorithm. They

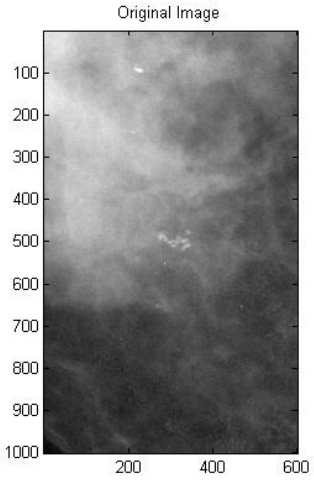

(a) Original Image

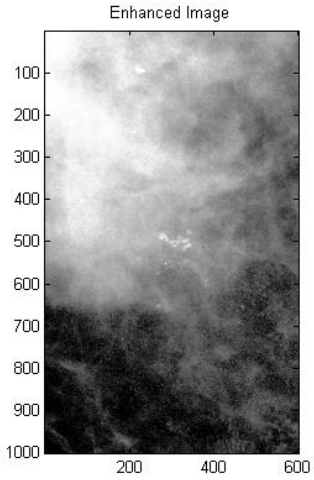

(b) Enhanced Image

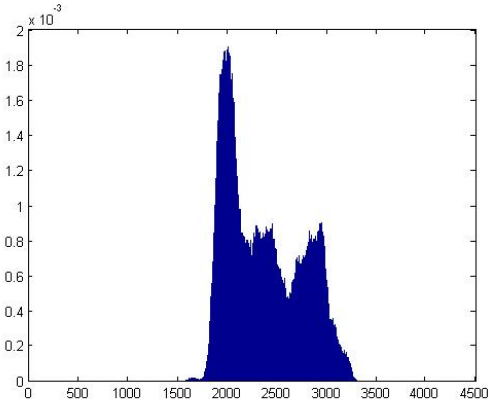

(c) Original Histogram

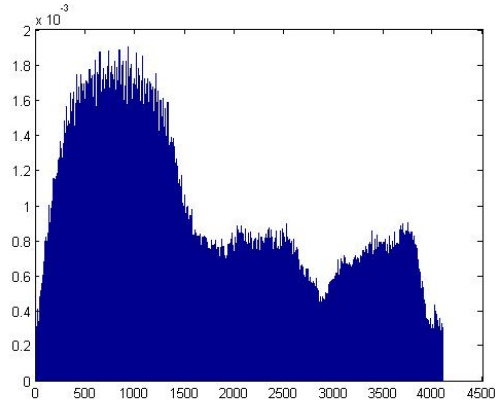

(d) Enhanced Histogram

Figure 2.1: An example of histogram equalization

apply weighting and thresholding scheme to clamp the histogram at an upper threshold and a lower threshold and then transform the values between these thresholds.

2.2 Wavelet based image enhancement

Wavelet has been considered a powerful tool to decompose a signal into multiple subbands. Recently, some researchers have proposed image enhancement methods based on wavelet. First, decompose the image into various subbands. After the decomposition, modification of wavelet coefficients at various subband is done to denoise the signal or enhance the contrast. The enhanced image is reconstructed from the modified wavelet coefficients.

A. Laine et.al [14] first applied it in mammogram contrast enhancement. A three-level dyadic wavelet is used to decompose the mammographic images and followed by a piecewise enhancement function called functional mapping to enhance the contrast and remove the noise at the same time. Fig 2.2 illustrates this general scheme. *DWT* is the discrete wavelet transform while *IDWT* is the inverse discrete wavelet transform. $x(n)$ and $y(n)$ are original signal and processed signal, respectively. The original signal is decomposed by the *DWT* and then processed by thresholding scheme or nonlinear function mapping and reconstructed with the *IDWT* to produce the denoised or enhanced signal/image.

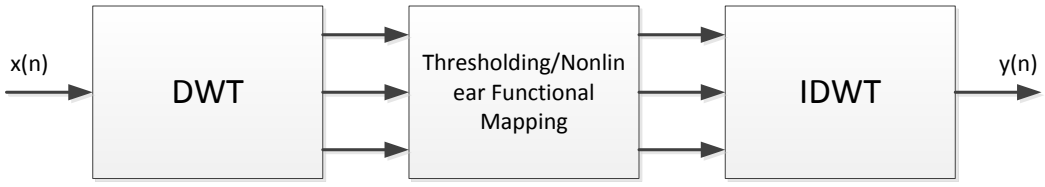

Figure 2.2: Wavelet based scheme

Soft-thresholding and hard-thresholding are the two main wavelet thresholding methods. D.L. Dohono [11] proposed a global thresholding scheme for removing the noise:

1. Hard-thresholding
$$y = \begin{cases} x & \text{if } |x| > T, \\ 0 & \text{Otherwise .} \end{cases} \tag{2.3}$$
2. Soft-thresholding
$$y = \begin{cases} sgn(x) * (|x| - T) & \text{if } |x| > T, \\ 0, & \text{Otherwise .} \end{cases} \tag{2.4}$$

Here, $T = \sigma\sqrt{2\ln N}$ is a popular candidate of that predefined threshold selection. [12] σ is the estimated standard deviation of noise and N is the length/size of signal. For the convenience, wavelet-HT and wavelet-ST are used to represent the wavelet hard thresholding method and wavelet soft thresholding method, respectively.

In [14], the authors proposed an effective nonlinear enhancement method, functional mapping (NLFM). Functional mapping is a simple piecewise function which is defined as:

$$y = \begin{cases} x-(K-1)T & \text{if } x < -T, \\ Kx & \text{if } |x| \leq T, \\ x+(K-1)T & \text{if } x > T. \end{cases} \tag{2.5}$$

For hard/soft thresholding and nonlinear functional mapping, x is the input signal and y is the denoised signal. The variables x and y are the wavelet coefficients and T is the predefined threshold. K is a gain to help enhance the signal. All these parameters can be different with respect to different wavelet subband.

As it is argued in [14], this nonlinear enhancement function meets the following rules:

Rule 1: Low contrast area is enhanced more than the area of high contrast.

Rule 2: Sharp edges will not be blurred.

Rule 3: Monotonicity keeps the position of local extrema unchanged without creating new extrema

Rule 4: Antisymmetry preserve phase polarity.

This enhancement method can enhance the image locally without blurring the edges. Also, it is reported in [14] that this nonlinear algorithm includes unsharp masking as a subset.

2.3 Empirical Mode Decomposition

The EMD method [15] is an algorithm which decomposes the signals into a number of amplitude and frequency modulated (AM/FM) zero mean signals named Intrinsic Mode Functions (IMFs). EMD is considered a subband decomposition method like wavelet, but the basis functions of EMD are signal-dependent. EMD derives the basis signal from the origianl signal. Since EMD decomposes the signal based on local characteristics of the data, it is a useful tool to process those nonlinear and non-stationary signals.

The EMD decomposes signal into a sum of IMFs that satisfy following two conditions:

1. The number of zero crossings and the number of local extrema must be the same or off by at most one.
2. The mean defined by the average of the local maxima envelop and local minimum envelop must be zero.

Once an IMF is found, the residue function is determined by subtracting the current IMF from the previous residue. For instance, let $y(n)$ be a 1D signal and $y_i(n)$ be the i^{th} IMF where $i \in Z^+$. The $i+1^{th}$ IMF $y_i(n)$ is determined by the sifting procedure. The sifting procedure determined by the following:

1. determine the maximum envelop by a spline interpolation of the local maxima, $y_{max}(n)$;
2. determine the minimum envelop by a spline interpolation of the local minima, $y_{min}(n)$;
3. the mean signal is $\bar{y}(n) = \dfrac{y_{max}(n) + y_{min}(n)}{2}$;
4. subtract $\hat{y}(n)$ from $y(n)$, $\hat{y}(n) = y(n) - \bar{y}(n)$;
5. if $\hat{y}(n)$ satisfies those two IMF conditions listed above, then the iteration stops and $\hat{y}(n)$ defines the IMF of $y(n)$. Otherwise, repeat this sifting process for $y(n) = \hat{y}(n)$.

The first residue is defined as:

$$r_1(n) = y(n) - y_1(n). \tag{2.6}$$

For other $i \neq 1$ the residue $r_i(n)$ is:

$$r_i(n) = r_{i-1}(n) - y_i(n). \tag{2.7}$$

After sifting, the signal can be reconstructed as a summation of all the IMFs and residue:

$$y(n) = \sum_{i=1}^{N} IMF_i(n) + r_N(n). \tag{2.8}$$

Some researchers have developed signal denoising algorithm based EMD with thresholding, which is similar to the wavelet shrinkage denoising technique. The main difference between wavelet shrinkage and EMD-shrinkage is that these thresholding methods are applied to each IMF instead of different wavelets subbands.

Furthermore, researchers [21] argued that there will always be part of IMFs whose absolute amplitude will drop below any nonzero threshold in the proximity of the zero-crossing even in noiseless case. Therefore, they developed a new thresholding scheme called interval thresholding.The new thresholding scheme is based on if the signal interval (signal between successive zero-crossings) is noise-dominant or signal-dominant. If the extrema in this interval lies below the threshold, this interval is considered as noise-dominant and vice versa. The following formulas define this new thresholding:

$$\widehat{IMF}_j(\mathbf{z^i}) = \begin{cases} IMF_j(\mathbf{z^i}) & \text{if } |IMF_j(r^i)| > T_i, \\ 0 & otherwise \end{cases} \tag{2.9}$$

where $\widehat{IMF}_j(\mathbf{z^i})$ is the denoised i^{th} IMF while $IMF_j(\mathbf{z^i})$ is original one. And j means the j^{th} interval, r represents the extrema in the j^{th} interval, in other words, extrema lies between two successive zero-crossings of IMF. The threshold T_i is also redefined in paper [21]. The final denoised signal will be reconstructed by adding all the denoised IMFs and residue together. This EMD based signal denoising method is called EMD-IT. Similarly, EMD-based enhancement can use nonlinear functional mapping to achieve contrast and detail enhancement.

CHAPTER 3: METHODOLOGY

In this chapter, the detailed methodology of image enhancement for mammographic images will be presented including the illustrations of the SBF and the LP. Also the objective measurement for image enhancement, Enhancement Measurement by Entropy (EME), will be discussed.

As it is mentioned in the previous chapter, noise existence is a big issue for mammogram images. Thus, I will start from signal denoising in order to enhance the mammogram images. In this thesis, one dimensional signal denoising algorithm will be discussed.

3.1 1D Signal Denoising

Typically, the noisy signal is defined as a noise-free signal with added noise signal:

$$y(n) = x(n) + \eta(n)$$

where $y(n)$ is the noisy signal, $x(n)$ is the noise-free signal and $\eta(n)$ is the pure noise signal. In order to recover the noise-free signal from the noisy signal, signal denoising algorithm will be applied to remove or reduce the additive noise.

Previously proposed signal restoration methods include linear filtering such as a moving average and Weiner filtering [27], non-linear filters such as various adaptive median and regression filters [25, 26], wavelet thresholding [12], *etc.* Since white noise has a constant spectrum, the current state of the art denoising ideology is to decompose the noisy signal into various subbands. A thresholding of each subband decomposed signal is claimed to provide beneficial denoising [11, 28].

I developed a new signal denoising algorithm based on the SBF. The 2D SBF proposed in [2] was shown to provide a reliable method to contrast enhance ultrasound images.

My new algorithm adds two extra thresholds to the basic SBF. I call this algorithm SBF with thresholds(SBFT). The SBFT algorithm is applied as follows.

Let $y(n)$ be a length N noisy signal.

Step 1: Set iteration indices $i, j = 0$ and $y_{i,j}(n) = y(n)$.

Step 2: Set iteration limits $\lambda_1, \lambda_2 > 0$, thresholds $T_{i,1}, T_{i,2} \geq 0$ for $i = 0, 1, 2, \ldots, \lambda_2$, and convergence criteria $\varepsilon > 0$.

Step 3: Each iteration j (j starts at one) begins by determining the set of locations of local maxima (peaks) and local minima (valleys). The locations of these extrema are defined by the set

$$\mathcal{N}_E = \{(n,m) \mid y_{i,j-1}(n) \text{ meets condition 1 or 2 }\}$$

Condition 1: $y_{i,j-1}(n) > y_{i,j-1}(n-1)$ and $y_{i,j-1}(n) > y_{i,j-1}(n+1)$

Condition 2: $y_{i,j-1}(n) < y_{i,j-1}(n+l)$ and $y_{i,j-1}(n) < y_{i,j-1}(n+1)$

Step 4: Without using the local extrema values, samples within a length L window centered at $y_{i,j-1}(n)$ are used to determine the local mean. These extrema may be replaced with the local mean values. That is for $n \in \mathcal{N}_E$ the local mean is computed as:

$$\bar{y}_{i,j-1}(n) = \frac{1}{L-1}\left(\left(\sum_{l=-\lfloor \frac{L}{2} \rfloor}^{\lfloor \frac{L}{2} \rfloor} y_{i,j-1}(n+l)\right) - y_{i,j-1}(n)\right)$$

where $\lfloor \cdot \rfloor$ is the greatest integer function.

Step 5: The minimum and maximum values within the length L window centered at $y_{i-1}(n)$ are determined

$$m = \min\left(\left\{ y_{i,j-1}(n+l) \;\middle|\; l = 0, \pm 1, \pm 2, \pm \left\lfloor \frac{L}{2} \right\rfloor \right\}\right)$$

and

$$M = \max\left(\left\{ y_{i,j-1}(n+l) \;\middle|\; l = 0, \pm 1, \pm 2, \pm \left\lfloor \frac{L}{2} \right\rfloor \right\}\right).$$

Step 6: The outlier maybe replace according to

$$y_{i,j}(n) = \begin{cases} y_{i,j-1}(n) & \text{if } |M-m| \geq T_{i,1} \text{ or} \\ & \quad |\bar{y}_{i,j-1}(n) - y_{i,j-1}(n)| \geq T_{i,2} \\ \bar{y}_{i,j-1}(n) & \text{otherwise.} \end{cases}$$

Step 7a: If $j < \lambda_1$ and convergence in the Cauchy sense is not attained, that is

$$\sum_{n=0}^{N-1} |y_{i,j-1}(n) - y_{i,j}(n)| > \varepsilon, \tag{3.1}$$

then j is incremented by one and another iteration, starting from Step 3, is performed.

Step 7b: If $j = \lambda_1$ or Cauchy convergence, contrary to equation (3.1), is attained, then when $i < \lambda_2$, i is incremented by one, $j = 0$, and

$$y_{i,j}(n) = y_{i-1,\lambda_1}(n) * h(n)$$

where $h(n)$ is a simple low pass filter. The process continues starting at Step 3.

Step 8: The algorithm stops when $i = \lambda_2$. An approximation of the noise free signal is produced as

$$\widehat{y}(n) = y_{\lambda_2,\lambda_1}(n).$$

Experiments to compare the various wavelet, EMD-IT, and proposed SBFT methods were performed. The wavelet-ST, wavelet-HT, ideal wavelet methods were from the WaveLab [29] library of Matlab functions. Four WaveLab noise free signals used were Piece-Regular (PR), Piece-Polynomial (PP), Blocks (BL), and Doppler (DP) of length 1024 were generated by the WaveLab MakeSignal.m function. Noisy signal were created by adding Gaussian noise with standard deviations (σ) of 5, 5, 1, and 0.1 to noise free PR, PP, BL, and DP signals, *resp.*.

The quadrature mirror filter bank in the wavelet transforms used a length 8 Daubechies wavelet. Both the wavelet-ST and wavelet-HT used a four level (five subbands) decomposition. The Donoho threshold, $T = \sigma\sqrt{\ln(2 \times 1024)}$, was applied in the HT and ST operations, where σ is the standard deviation of the additive noise. The ideal wavelet denoising

Table 3.1: SBFT Parameters

	PR	PP	BL	DP
λ_1	3	45	30	2
$T_{0,1}$	21	70	4	0.34
$T_{0,2}$	18	60	2	0.35
$T_{1,1}$	12	40	2.4	0.29
$T_{1,2}$	5	25	1.4	0.13

method adjusts the applied threshold based on the noise free signal. In my research, ideal wavelet denoising method is set as a standard for other methods. In other words, ideal wavelet denoising method provide a psuedo-upper bound the on the attainable Signal to Noise Ratio (SNR).

The EMD-IT denoising software was attained from [30]. As it is discussed in previous chapter, the EMD-IT employed a new thresholding operation, called interval threshold, to the IMF decomposition. The threshold parameters of EMD-IT in equation (2.9) were manually optimized using a greedy method to provide the largest possible SNR.

The proposed SBFT method used a length $L = 9$ window to perform the local averaging in Step 4. The convergence parameter in equation (3.1) is set to $\varepsilon = 0.01$ and iteration parameter $\lambda_2 = 2$. The iteration parameter λ_1 and the threshold parameters used in the proposed SBFT to denoise each signal are given in Table 3.1 and were determined from a greedy search. The low pass filter in Step 7b was a simple three point averaging filter.

The SNR of the denoised signal is used to evaluate the performance of each method. The SNR of a restored or noisy signal $\widehat{y}(n)$ is defined as

$$\text{SNR}\left\{\widehat{\mathbf{y}}\right\} = 20\log_{10}\left(\frac{\|\mathbf{x}\|}{\|\mathbf{x}-\widehat{\mathbf{y}}\|}\right) \text{ dB}$$

where $\|\cdot\|$ denotes the l_2-norm and $x(n)$ is the noise free signal. The SNRs of the noisy signal and each denoising method tested in these experiments are given in Table 3.2. It is not surprising that the unpractical ideal wavelet method, which requires the noise free signal as an input parameter, provides the best SNR in all but the BL signal. In general the wavelet-

ST, wavelet-HT, and EMD-IT does provide significant denoising improvements with an increase in SNR over the unprocessed SNR in all cases except the wavelet-ST degraded the SNR in the BL signal. The proposed SBFT provides over 2 dB improvement over the wavelet-ST, wavelet-HT, and EMD-IT methods in restoring the PR and PP signals and over 3 dB improvements in restoring the BL signal. The SNR of the proposed SBFT method is about 2 dB less than the wavelet-HT method and the EMD-IT method in denoising the DP signal. Thus, the DP example provides evidence that the wavelet-HT and EMD-IT are more robust when the signal is strictly band limited. In all other cases SBFT achieved superior performance. The results of each restoration method applied to the four tested signals are shown in Fig. 4.1. Noise-free signals are shown in blue while noisy signals are in black. Signals showed in red refer to those denoised signals.

An overview of the wavelet HT, wavelet-ST, and EMD-IT methods is provided. The wavelet and EMD methods rely on a subband decomposition and subsequent HT or ST to restore a signal corrupt with additive noise. The SBFT incorporates a thresholding operation into the SBF algorithm to preserve a signal's peaks and valleys, while the additive noise is removed. Experiments using the length 1024 PP, PR, BL, and DP signals were performed. The results of these experiments show the proposed SBFT provided in excess of 2 dB SNR improvement over the wavelet-ST, wavelet-HT, and EMD-IT methods on the PR, PP, and BL signals. In the PP restoration the SBFT nearly attained the same SNR as the unpractical ideal wavelet method. In the BL example the SNR of SBFT exceeds the SNR of the ideal wavelet method and SBFT provides over 3 dB improvements over the other methods. When restoring the band limited DP signal, the SBFT did not perform on par with wavelet-HT and EMD-IT where the subband decomposition may have aided these methods. These experiments provide evidence that the SBFT may be a more robust denoising method than the other current state of the art methods with certain signals.

In contrast to SBFT, a 1D example of the SBF is shown in Fig 3.2. As it is discussed above, SBFT has been proved to be a good method to denoise certain type of signal. The original noisy signal is shown in Fig 3.2 as the black plot. The result of the SBF applied

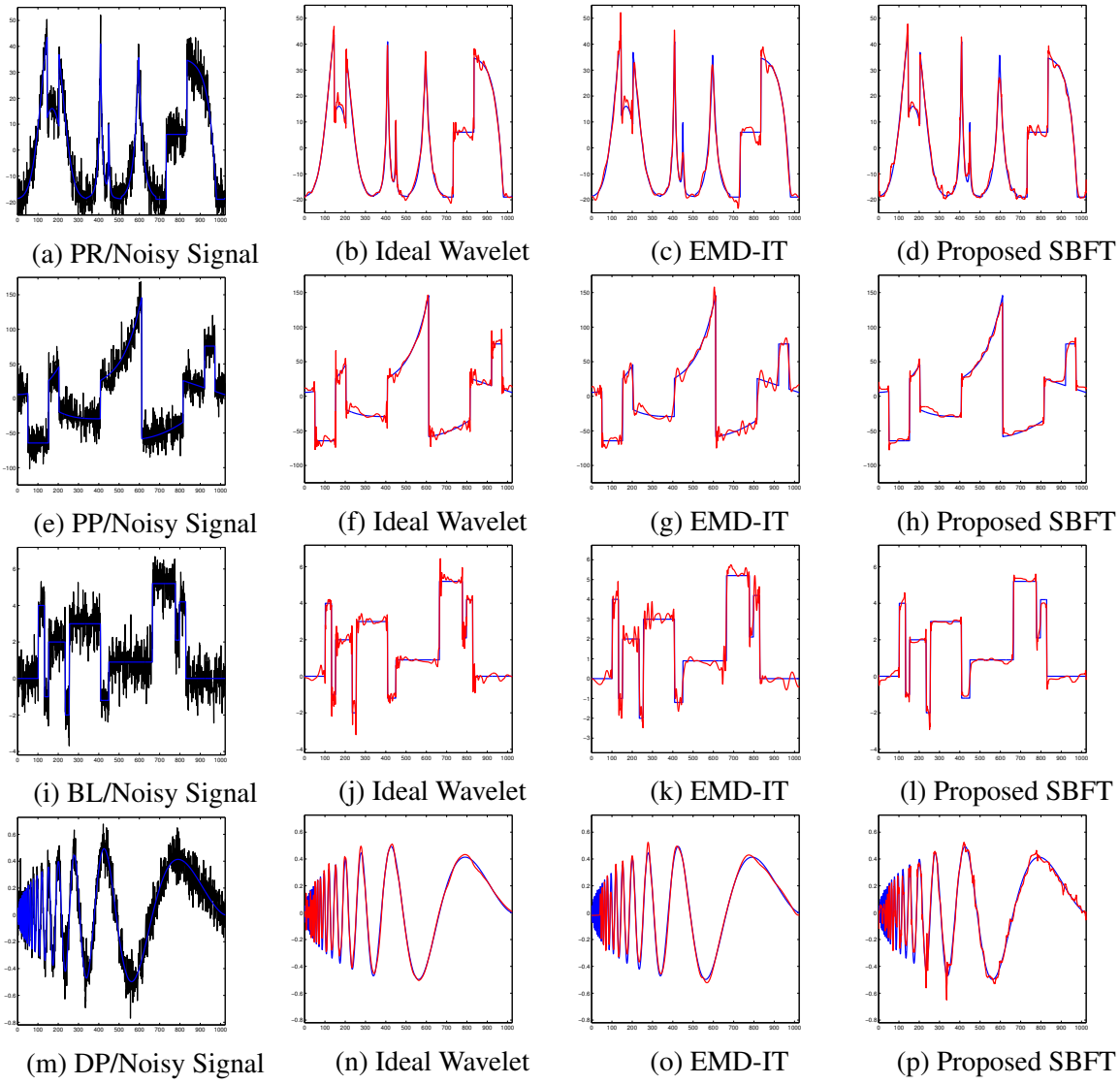

(a) PR/Noisy Signal (b) Ideal Wavelet (c) EMD-IT (d) Proposed SBFT

(e) PP/Noisy Signal (f) Ideal Wavelet (g) EMD-IT (h) Proposed SBFT

(i) BL/Noisy Signal (j) Ideal Wavelet (k) EMD-IT (l) Proposed SBFT

(m) DP/Noisy Signal (n) Ideal Wavelet (o) EMD-IT (p) Proposed SBFT

Figure 3.1: Noise free (blue) PR, PP, BL, DP, and noisy signals (black) and results (red) from various denoising techniques.

Table 3.2: Quantitative SNR (dB) Improvements

	WaveLab Signal			
Method	PR	PP	BL	DP
unprocessed	11.30	10.49	10.05	9.65
wavelet-ST	12.24	16.13	9.61	11.42
wavelet-HT	18.05	12.61	14.89	18.31
EMD-IT	18.26	16.24	16.48	18.51
SBFT	20.50	18.53	**19.64**	16.37
Ideal Wavelet	**22.83**	**18.71**	19.59	**20.58**

to the noisy signal is shown as the red plot in Fig 3.2. The red plot indicates that almost all the noise has been removed. However, the peaks are adversely diminished. These sharp peaks might indicate the location of MCs, which should be enhanced. Hence, this adversity will provide a means to isolate the fine details of an image, in which to apply enhancement. And, in [3], SBF was utilized in a background subtraction method. Resulting from all these reasons, a three level Laplacian Pyramid(LP) is proposed in this thesis to enhance the mammogram images.

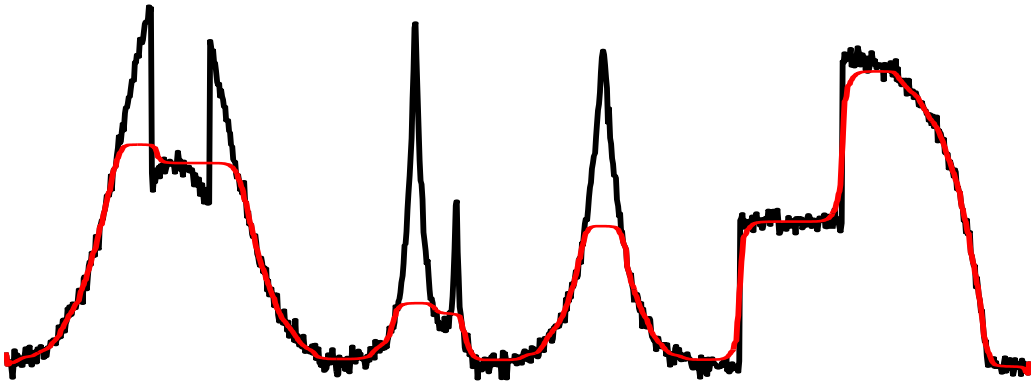

Figure 3.2: Example of 1D SBF.

3.2 The Proposed Image Enhancement Method

Fig 3.3 shows the block diagram of the proposed image enhancement method. It is easy to find that the whole enhancement method is generally divided in to two main parts: SBF based LP and NLFM. Our early research [3] indicates that the SBF filtered mammographic image is a good approximation of image background. In other words, the details we want to enhance, like MCs, can be found in the difference image between the original image and SBF image.

Hence, 2D SBF is used to substitute the low-pass filter in conventional LP to extract all the details to be enhanced. WThe NLFM has been proven to be a good local enhancement scheme in [14]. It shows even better enhancement in our proposed method.

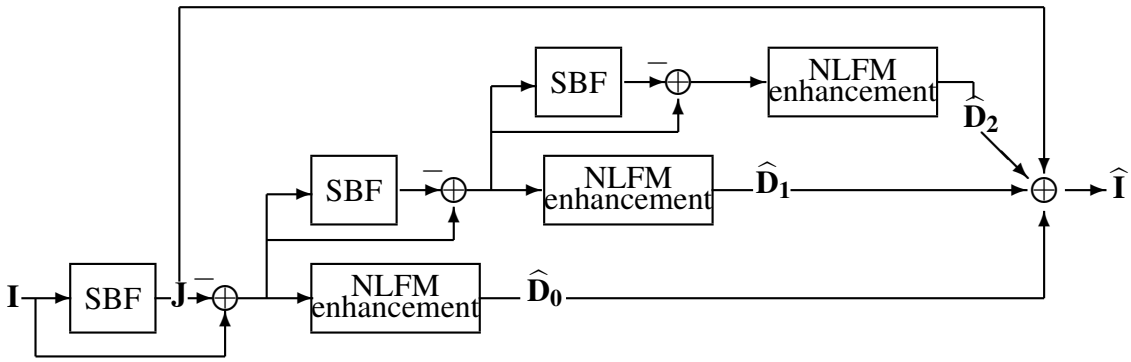

Figure 3.3: Proposed image enhancement scheme.

3.2.1 Squeeze Box Filter

Now we are dealing with 2D signal, image. So 2D SBF will be used. The SBF computes the nonstationary local mean by iteratively removing outliers. In 2D, image pixel outliers are defined to be local minimums and local maximums determined from a 3×3 window. After outlying pixel values are found, each outlier is replaced by a local mean determined from a $L \times L$ window centered on the outlying pixel. The outlier pixel value is not used in computing the local mean. After all the outliers are replaced by the local means, the process is repeated until a predetermined number of iteration is reached or until convergence is attained.

The two dimensional SBF algorithm is applied as follow. Let $I(n,m) = J_0(n,m)$ be a $N \times M$ image.

Step 1: Each iteration i (i starts at one) begins by determining the set of locations of local maxima (peaks) and local minima (valleys) of the image. The locations of these extrema are defined by the set

$$\mathcal{N}_E = \{(n,m) \mid J_{i-1}(n,m) \text{ meets condition 1 or 2 } \}$$

Condition 1: $J_{i-1}(n,m) > J_{i-1}(n+l,m+k)$

Condition 2: $J_{i-1}(n,m) < J_{i-1}(n+l,m+k)$

for all $l,k = -1,1$.

Step 2: Without using the local extrema values, samples within a $L \times L$ window centered at $J_{i-1}(n,m)$ are used to determine the local mean. These extrema will be replaced with the local mean values. That is for $(n,m) \in \mathcal{N}_E$ the local mean is computed as:

$$J_i(n,m) = \frac{1}{(L \times L) - 1} \left(\left(\sum_{l,k=-\lfloor \frac{L}{2} \rfloor}^{\lfloor \frac{L}{2} \rfloor} J_{i-1}(n+l, m+k) \right) - J_{i-1}(n,m) \right)$$

where $\lfloor \cdot \rfloor$ is the greatest integer function.

Step 3: If a predetermined maximum number of iterations is not exceeded and convergence in the Cauchy sense is not attained, that is

$$\sum_{n,m=0}^{N-1,M-1} |J_{i-1}(n,m) - J_i(n,m)| > \varepsilon$$

for some small predefined $\varepsilon > 0$, then another iteration is performed. If the maximum number iterations is reached or Cauchy convergence is attained, then the algorithm stops and the output image $\mathbf{J} = \mathbf{J}_i$.

Paper [2] also discusses the choice of the size of the neighbor window. As it is discussed, a large neighborhood will produce a local mean close to the mean of the homogeneous region. However, if the neighborhood size is too large will go past homogeneous region, a misleading value will be produced. On the other side, a small window size may require more iterations to remove those outliers. In order to make SBF work appropriately with respect to different applications selection of the optimal neighborhood size becomes very important.

3.2.2 Laplacian Pyramid

The LP is a decomposition of the original image into a hierarchy of images such that each level corresponds to a different band of image frequencies. [17]

SBF can be applied to extract the details of the mammographic images and SBFT can recover the signal from significant noise. It is reasonable to use SBF algorithm to substitute the simple low-pass filter in the LP to extract those details i.e. MCs efficiently

in each level of LP. As it is shown in Fig 3.3, after subtracting the SBF smoothed image. NLFM is applied to amplify features that were obscured in the original image without distorting edges. The final detail enhanced image is produced by summing the original SBF image with those enhanced difference images. The result is a contrast enhanced image with visually preserved details.

3.3 Enhancement Measure by Entropy

Direct image enhancement requires a suitable image enhancement measure which should provide a quantitative evidence whether the image is enhanced and also an indicator on how much it is enhanced. S.S. Agaian et al. [18] proposed a new quantitative measurement of image enhancemen EME. EME is defined based on the definition of image contrast. Though there are several various definitions of image contrast, EME introduces human visual concept to measure the enhancement. Therefore, EME is believed to be a good objective measurement of image enhancement especially contrast enhancement. Two definitions of contrast measure have been widely-used for simple patterns: Michelson [19] and Weber's Contrasts. They are defined as follows.

$$Michelson\ \ Contrast = (L_{max} - L_{min})/(L_{max} + L_{min}) \tag{3.2}$$

$$Weber\ \ Contrast = L_{max}/L_{min} \tag{3.3}$$

where L_{max} and L_{min} are the local maximum and minimum grayscale value of image respectively. The authors in [18] proposed a new form of EME which is defined using entropy. The following two EMEs are based on Michelson law-based contrast and Weber Law-based contrast respectively:

$$EME = \frac{1}{k_1 k_2} \sum_{l=1}^{k_1} \sum_{k=1}^{k_2} 20 \ln \frac{I_{max;k,l} + I_{min;k,l}}{I_{max;k,l} - I_{min;k,l} + c} \tag{3.4}$$

$$EME = \frac{1}{k_1 k_2} \sum_{l=1}^{k_1} \sum_{k=1}^{k_2} 20 \ln \frac{I_{max;k,l}}{I_{min;k,l} + c} \tag{3.5}$$

where k_1, k_2 are local neighborhood size, $I_{max;k,l}$ and $I_{min;k,l}$ are the maxima and minima value of local neighborhood respectively. The parameter c is a small constant equal to 0.0001 to avoid dividing by 0. Generally, high EME value indicates high contrast. However, when Michelson's law is applied the lower the EME value means higher contrast. It is obvious that high contrast neighborhoods give a high EME value while EME value goes down for homogeneous neighborhood. [20]

CHAPTER 4: EXPERIMENTAL RESULTS AND DISCUSSIONS

In order to test the proposed image enhancement method, images from four DDSM cases were selected. There is only one malignant, pleomorphic and clustered MC ROI for each case.

The experiment uses a three level LP as shown in Fig. 3.3. Each enlarged ROI image is SBF processed until the Cauchy convergence was below $\varepsilon = 0.0001$ or until 200 iterations were completed. The NLFM enhancement used $T_\lambda = 100$ for $\lambda = 0, 1, 2$ and $W_0 = 2$, $W_1 = 3$, and $W_2 = 4$. The enhancement method described in [14] applies NLFM enhancement to the two level wavelet transform decomposed image then reconstructs the image using the NLFM enhanced wavelet images. The wavelet decomposed images are NLFM enhanced using $K = 2$ and $T = 0.02 \times \max\{x\}$ for two scales [14]. A length eight Daubechies wavelet was used in the two level DWT.

The first row of Fig. 4.1 shows those four original enlarged DDSM ROIs while the enhancement results of the proposed method are shown in the third row. We can find easily that the MCs and other details especially edges around the MCs are more visible in the LP-NLFM enhanced images. In addition, the fine details of the breast tissue that were clouded in the original images are clearer visibly. Images in the second row show the enhancement results of Wavelet-NLFM. All these images processed by Wavelet-NLFM [14] do not appear obvious difference from the original images. In other words, the Wavelet-NLFM does not enhance the mammogram image's ROI very well. The quantitative results also support this observation.

The EME based on the Michelson contrast, *i.e.* modulation, as described in Chapter 3 is used to quantify the enhancement results. EME is proposed to measure the local detail enhancements in [18]. In the denominator of equation (3.4), $I_{max} - I_{min}$ defines the local pixel intensity difference. Thus, larger value in the denominator means smaller contrast in

Table 4.1: EME Results

DDSM Case	Original	wavelet-NLFM	LP-NLFM
A_1153.1_LEFT_CC	72.53	71.06	**40.73**
A_1214.1_LEFT_CC	70.67	69.37	**37.06**
A_1220_1.RIGHT_CC	64.07	62.76	**42.72**
A_1223_1.LEFT_CC	67.42	65.79	**32.79**

an 8×8 window. Furthermore, lower EME score would indicate better detail or contrast enhancement.

Table 4.1 lists the EME scores of Wavelet-NLFM [14] enhancement results and proposed LP-NLFM enhancement results respectively. EME scores of all four DDSM cases enhanced by the proposed LP-NLFM method are lower than scores of the original and wavelet-NLFM enhanced images. It is evident that the proposed LP-NLFM enhancement method may provide better visual enhancement than the wavelet-NLFM method from this abbreviated experiment.

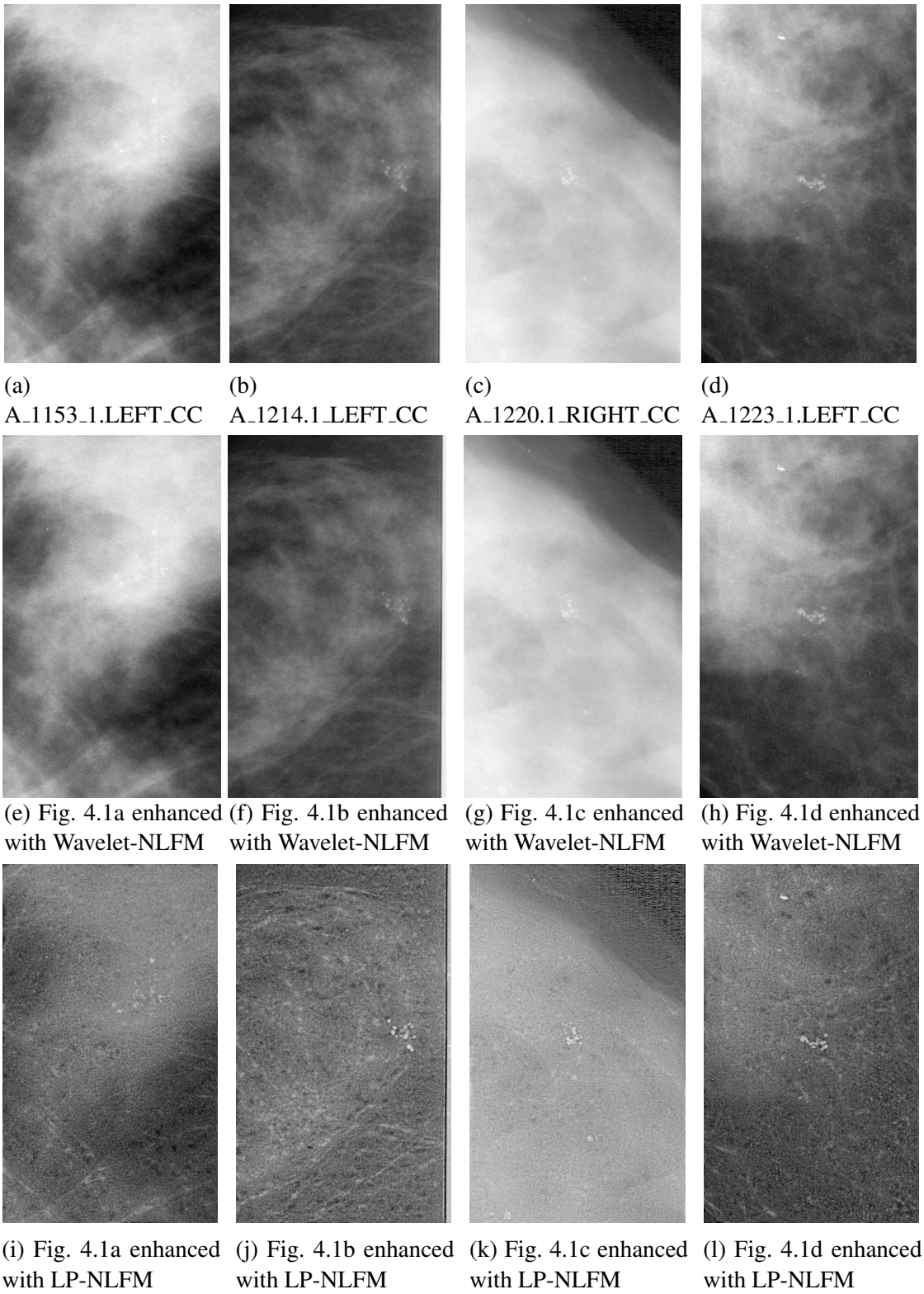

(a) A_1153_1.LEFT_CC (b) A_1214.1_LEFT_CC (c) A_1220.1_RIGHT_CC (d) A_1223_1.LEFT_CC

(e) Fig. 4.1a enhanced with Wavelet-NLFM (f) Fig. 4.1b enhanced with Wavelet-NLFM (g) Fig. 4.1c enhanced with Wavelet-NLFM (h) Fig. 4.1d enhanced with Wavelet-NLFM

(i) Fig. 4.1a enhanced with LP-NLFM (j) Fig. 4.1b enhanced with LP-NLFM (k) Fig. 4.1c enhanced with LP-NLFM (l) Fig. 4.1d enhanced with LP-NLFM

Figure 4.1: The results from four DDSM malignant, pleomorphic, and clustered MC cases. Figs. 4.1a- 4.1d are the original unprocessed enlarged ROIs. Figs. 4.1e- 4.1h are Wavelet-NLFM enhanced enlarge ROIs. Figs. 4.1i- 4.1l are LP-NLFM enhanced enlarge ROIs.

CHAPTER 5: CONCLUSION AND FUTURE WORK

E. A. Sickles M.D., Ph.D. showed clinically the existence of MC of irregular shape to be a reliable indicator of malignant breast cancer in [33]. This thesis proposed a novel image enhancement method which can assist radiologists or improve computer aided detection and diagnosis methods in the early stage of breast cancer detection. Especially this proposed image enhancement algorithm can be applied to help radiologist(s) detect irregular shaped MCs.

The proposed image enhancement method is based on a three level LP decomposition of a mammogram image. The multi-level LP uses SBF instead of typical low pass filtering. These LP difference image contain important structural and textural details of the mammogram image. Starting from the original image, SBF is applied to process the image and subtract the SBF image from the original image to produce the difference image. Then the current difference image will be used as the original image for the next level. After LP, all the difference images produced in LP are enhanced by applying NLFM operation. The sum of the first SBF image and all the enhanced difference images produce the final enhanced image where fine structures of the breast tissue, which were obscured in the original unprocessed image, are visibly clearer.

The experimentation results reported in Chapter 4 show improvement in image contrast and enhanced structural details of mammogram images. Moreover, MCs, tissue structure and other fine details are made more visible. One main advantage of proposed LP-NLFM image enhancement is that the proposed method avoids the distortion of edges and preserve the shape of MCs. Therefore, this enhancement technique can be an effective tool to assist radiologists at an early treatable stage of detection and diagnosis of malignant breast cancer.

The EME performance metric using the Michelson contrast was used to quantify the

enhancement results. The EME measure was chosen since it has been claimed to indicate positive visual enhancements when viewing translucent objects based on human perception models. The experimentation in this thesis showed that the proposed LP-NLFM method produced visually better enhanced (lower EME scores) than applying NLFM on a wavelet decomposition. However, EME has been reported to be very sensitive to noise of the image. In other words, low EME scores in some cases do not mean high contrast enhancement because of the existence of significant noise. EME score can be considered as a weighted sum of entropies of local contrast of all the small windows. All of those weights are set the same in the basic EME. The future work may focus on use different weights considering different noise level in each local window to build a new EME definition.

Furthermore, my future research goal is to apply this novel image enhancement method to pre-process images acquired from fully digital modern clinical or research mammography systems and then test the classification method proposed in [4].

BIBLIOGRAPHY

[1] American Cancer Society, "Cancer Facts & Figures 2013," http://www.cancer.org/acs/groups/content/@epidemiologysurveilance/documents/document/acspc-036845.pdf, 2013 (accessed March 31, 2013).

[2] P. C. Tay, C. D. Garson, S. T. Acton, and J. A. Hossack, "Ultrasound despeckling for contrast enhancement," *IEEE Trans. Image Processing*, vol. 19, no. 7, pp. 1847–1860, July 2010.

[3] P. Tay and H. Shen, "A novel background subtraction method to detect microcalcifications ," Proc. 2012 *IEEE Southwest Symposium on Image Analysis and Interpolation*, pp. 141-144, Apr. 2012.

[4] P. Tay and Y. Ma, "A novel microcalcification shape metric to classigy regions of interests ," Proc. 2012 *IEEE Southwest Symposium on Image Analysis and Interpolation*, pp. 201-204, May. 2010.

[5] A. Rosenfeld and A.C. Kak, "Digital Picture Processing," Computer Science and Applied Mathematics, Academic Press, 1982.

[6] Q. Wang, and R.K. Ward, "Fast image/video contrast enhancement based on weighted thresholded histogram equalization," *IEEE Trans. Consumer Electronics.*, vol.51, no.4, pp. 757-764, May 2007.

[7] Y. T. Kim, "Contrast enhancement using brightness preserving bi-histogram equalization," *IEEE Trans. Consumer Electronics.*, vol.43, no.1, pp. 1-8, Feb. 1997.

[8] Y. Wang, Q. Chen and B. Zhang, "Image enhancement based on equal area dualistic sub-image histogram equalization method," *IEEE Trans. Consumer Electronics.*, vol.45, no.1, pp. 68-75, Feb. 1999.

[9] S. D. Chen and A. Ramli, "Minimum mean brightness error bi-histogram equalization in contrast enhancement," *IEEE Trans. Consumer Electronics.*, vol.49, no.4, pp. 1310-1319, Nov. 2003.

[10] M. Abdullah-AL-Wadud, M. Kahir, M. Dewan and O. Chae, "A dynamic histogram equalization for image contrast enhancement," *IEEE Trans. Consumer Electronics.*, vol.53, no.2, pp. 593-600, May 2007.

[11] D.L. Dohono, "De-noising by soft-thresholding," *IEEE Information Theory*, vol.41, no.3, pp. 613-627, 1995.

[12] S. Mallat, "A wavelet Tour of Signal Processing," 2nd edition New York: Academic, 1999.

[13] R. C. Gonzalez and R. E. Woods "Digital Image Processing," 2nd edition Pearson Education, 2002.

[14] A. Laine, J. Fan, and W. Yang, "Wavelets for contrast enhancement of digital mammography," *IEEE Engineering in Medicine and Biology*, pp. 536-550, Sep./Oct. 1995.

[15] N.E. Huang, Z. Shen, S.R. Long, M. Wu, H.H. Shih, Q. Zheng, N.C. Yen, C.C. Tung, and H.H. Liu, "The empirical mode decomposition and the Hilbert spectrum for nonlinear and non-stationary time series analysis," Proc. of The Royal Society, vol. 454, pp. 903-995, March 1998.

[16] H. Wang, Y. Chen, T. Fang, J. Tyan and N. Ahuja, "Gradient Adaptive Image Restoration and Enhancement," *IEEE Proc. Int. Conf. Image Processing*, pp. 2893–2896,Oct. 2006.

[17] P. Burt and E. Adelson, "The Laplacian Pyramid as a Compact Image Code," *IEEE Trans. Communications.*, vol.31, no.4, pp. 532-540, Apr. 1983.

[18] S. S. Agaian, B. Silver, and K. A. Panetta, "Transform coefficient histogram-based image enhancement algorithms using contrast entropy," *IEEE Trans. Image Processing.*, vol.16, no.3, pp. 741-758, Mar. 2007.

[19] A.A. Michelson, *Studies in Optics*, Chicago, IL: Univ. Chicago Press, 1927.

[20] T. Celik and T. Tjahjadi, "Contextual and Variational Contrast Enhancement," *IEEE Trans. Image Processing.*, vol.20, no.12, pp. 3431-3441, Dec. 2011.

[21] Y. Kopsinis and S. Mclaughlin, "Development of EMD-Based Denoising Methods Inspired by Wavelet Thresholding," *IEEE Trans. Signal Processing.*, vol.57, no.4, pp. 1351-1362, Apr. 2009.

[22] J. Tang, X. Liu and Q. Sun, "A Direct Image Contrast Enhancement Algorithm in the Wavelet Domain for Screening Mammograms," *IEEE Trans. Image Processing.*, vol.3, no.1, pp. 74-80, Feb. 2009.

[23] N. Petrick, H. CHan, B. Sahiner and D. Wei, "An Adaptive Density-Weighted Contrast Enhancement Filter for Mammographic Breast Mass Detection," *IEEE Trans. Medical Imaging.*, vol.15, no.1, pp. 59-67, Feb. 1996.

[24] P. Heinlein, J. Drexl and W. Schneider, "Integrated Wavelets for Enhancement of Microcalcifications in Digital Mammography," *IEEE Trans. Medical Imaging.*, vol.22, no.3, pp. 402-413, Feb. 1996.

[25] A. Restrepo and A. C. Bovik, "Adaptive trimmed mean filters for image restoration," *IEEE Trans. Acoust., Speech, Signal Processing*, vol.36, no.8, pp. 1326-1337, Aug. 1988.

[26] A. C. Bovik, T. Huang and Jr. D. Munson, "A generalization of median filtering using linear combinations of order statistics," *IEEE Trans. Acoust., Speech, Signal Processing*, vol.31, no.6, pp. 1342-1350, Dec. 1983.

[27] T. Kailath, "Equations of Wiener-Hopf type in filtering theory and related applications," Norbert Wiener: Collected Works, Vol.III, P.Masani, Ed., pp. 63-94, MIT Press, Cambridge, MA. 1983.

[28] H. Krim, D. Tucker, S. Mallat and D. Dohoho, "On de-noising and best signal representation," *IEEE Trans. Inform. Theory*, vol.45, no.7, pp. 2225-2238, Nov. 1999.

[29] "WaveLab 850," `http://www-stat.stanford.edu/~wavelab/Wavelab_850/index_wavelab850.html`, accessed Nov. 23, 2012.

[30] "Yannis Kopsinis - Software," `http://www.see.ed.ac.uk/~ykopsini/software.html`, accessed Nov. 23, 2012.

[31] "USF digital mammography home page," `http://marathon.csee.usf.ecu/Mammography/Database.html`, (accessed May 18, 2009).

[32] C. J. D´Orsi, *Illustrated Breast Imaging Reporting and Data System*, American College of Radiology, Reston, VA, 3rd edition, 1998.

[33] E. A. Sickles, "Breast calcifications: Mammographic evaluation," *Radiology*, vol.160, pp. 289–293, 1986.